A Novel Nanoporous Graphite Based on Graphynes: First Principles Structure and Carbon Dioxide Preferential Physisorption

Massimiliano Bartolomei*,† and Giacomo Giorgi‡

†*Instituto de Física Fundamental, Consejo Superior de Investigaciones Científicas (IFF-CSIC), Serrano 123, 28006 Madrid, Spain*

‡*Dipartimento di Ingegneria Civile ed Ambientale (DICA), The University of Perugia, Via G. Duranti 93, I-06125 Perugia, Italy*

E-mail: maxbart@iff.csic.es

Abstract

Ubiquitous graphene is a stricly 2D material representing an ideal adsorbing platform due to its large specific surface area as well as its mechanical strength and resistance to both thermal and chemical stresses. However, graphene as a bulk material has the tendency to form irreversible agglomerates leading to 3D graphitic structures with a significant decrease of the area available for adsorption and no room for gas intercalation. In this paper a novel nanoporous graphite formed by graphtriyne sheets is introduced: its 3D structure is theoretically assessed by means of electronic structure and molecular dynamics computations within the DFT level of theory. It is found that the novel layered carbon allotrope is almost as compact as pristine graphite but the inherent porosity of the 2D graphyne sheets and its relative stacking leads to nanochannels that cross the material and whose sub-nanometer size could allow the diffusion and storage of gas species. A molecular prototype of the nanochannel is used to accurately

determine first principles adsorption energies and enthalpies for CO_2, N_2, H_2O and H_2 within the pores. The proposed porous graphite presents no significant barrier for gas diffusion and it shows a high propensity for CO_2 physisorption with respect to the other relevant components in both pre- and post-combustion gas streams.

Keywords

carbon dioxide, carbon allotropes, graphynes, two-dimensional materials, physical adsorption, ab initio calculations

1 Introduction

The use of advanced porous materials for gas storage has recently received wide attention since they can help to provide solutions to growing concerns related to the anthropogenic carbon dioxide (CO_2) emissions which, in turn, are expected to rise considerably[1,2] if fossil fuels consumption will continue to dominate the energy scene.

In fact, porous materials could conveniently and efficiently reduce the carbon content in gas mixtures by exploiting the selective physical adsorption of CO_2 at the adsorbent's surface or within its pore network.

Activated carbons and zeolites are traditionally used to this scope and, more recently, promising adsorbents such as metal-organic frameworks (MOF)[3] have attracted much attention.

The crystalline structure of MOF implies noticeable advantages with respect to traditional porous materials: in fact, their regular and ordered porosity, together with tunable size and shape of the openings, has led to very high performances in gas uptake capacities.[4,5] However, their thermal stability as well as the vulnerability of the metal containing clusters to ligand substitution by water or other nucleophiles still represent not negligible shortcomings.

Therefore, investigations on alternative porous materials are highly advisable and, specifically, on those based on carbon since they provide a large specific surface area together with a low sensitivity to humidity as well as a low weight. As an example, very recently novel porous carbons have been synthesized[6] by means of a high temperature carbonization process of different MOF structures: very high CO_2 uptake capacities have been found which even improve those of the metal-organic precursors.

Ubiquitous graphene represents in principle the ultimate adsorbing carbon platform[7] due to its high surface area and mechanical strength, excellent thermal conductivity and good chemical stability, but the related gas uptake capacity is limited by its tendency to form irreversible agglomerates and intrinsic lack of pores. As a matter of fact bulk graphene tends to cluster in graphite platelets due to the large van der Waals forces between the large and planar basal planes and this leads to a significant decrease of the available surface area. Multi-layered graphenes or graphites could indeed lead to an enhanced gas storage after interlayer spacing expansion and/or activation. As an example, a larger separation between graphene-like planes has been obtained[8] from graphene oxide layers connected by molecular pillars but the related measured gas uptakes have been found quite lower than those predicted by the simulations and in any case not comparable with the best values reached with MOF materials.[4,5] Nevertheless, activated graphene-derived powders and structures heve been recently obtained[9,10] from exfoliated graphite oxide: these carbon materials have indeed shown exceptional gas adsorption properties which are comparable to those for MOFs having similar surface area.

The introduction of nanopores into graphene sheets is another effective possibility for improving their gas adsorption performances. In fact, in the last years two-dimensional (2D) materials similar to graphene but with regular and uniformly distributed subnanometer pores have been synthesized in large area films[11,12] by means of "bottom up" approaches. Among them γ-graphynes,[13,14] which are new 2D carbon allotropes formed by sp-sp^2 hybridized carbon atoms, are of particular interest and they feature triangular pores of sub-nanometer

size. In fact, their recent synthesis[12,15] has triggered important theoretical studies devoted to their application as effective single-layer membranes for gas separation and water filtration technologies.[16–20]

In addition to their use as sieving platforms, graphynes could be also promoted as adsorbents since the 2D sheets can be used as building blocks to construct novel graphyne-based 3D porous structures.[21–23]

As a matter of fact, we have recently shown[24] by means of a theoretical investigation that multi-layer γ-graphynes are more suited than graphene for the physical adsorption of molecular hydrogen (H_2). In particular, those based on graphtriyne layers (see Fig. 1), which are formed by phenyl rings fully interconnected by chains of three conjugated C-C triple bonds, can allow both H_2 intercalation and its diffusion through the carbon material and the computed adsorption energies inside the pores are almost doubling the related estimations[25–27] for the adsorption on pristine graphene. The size of the involved triangular pores (pore width below 0.7 nm) suggests they could be also effective to host molecules larger than H_2 and therefore their affinity for CO_2 physisorption can be postulated and it is worth to be further investigated.

In this work we first aim to correctly determine the 3D structure of a novel nanoporous graphite composed of stacked graphtriyne layers. Then, its capability for the preferential adsorption of CO_2 with respect to other gases such as nitrogen, water and hydrogen is theoretically addressed.

2 Computational Methods

The calculations for the graphtriyne 3D structure have been obtained by means of density-functional theory (DFT), as implemented in the VASP code,[28] within the generalized gradient approximation (GGA) of Perdew, Burke, and Ernzerhof (PBE).[29] The Blöchl all-electron projector-augmented wave (PAW) method,[30,31] with an energy cutoff of 750 eV and a $2s^2$

$2p^2$ electron valence potential for carbon, has been employed. A periodic model has been first considered for the graphtriyne isolated monolayer with an initial supercell (see Fig. 1) constituted by 48 C atoms with in-plane lattice parameter a = 12.035 Å and b = 20.841 Å, and with a sufficient vacuum amount to avoid spurious interaction between layers along the direction normal to the ab plane. According to the large size of the parameters, we have sampled the Brillouin zone (BZ) with a 5x4x1 Gamma centred mesh. Then a periodic model for the graphtriyne isolated bilayer with 48 atoms per layer (96 C atoms) has been taken into account in order to study the bilayer interaction energy. Keeping the supercell lattice parameters fixed to the initially optimized values, by means of single point calculations, we have progressively slided the top layer upon the bottom one along both a and b directions, respectively(see Fig. 1), at a fixed interlayer distance R= 3.45 Å which has been previously found[24] to be the optimal one for the bilayer interaction.

The computed energies have been corrected by two- and three-body dispersion contributions including the Becke-Johnson damping scheme[32] and an Axilrod-Teller-Muto three-body term,[33] as implemented in the $dftd3$ program of Grimme et al.[34]

Moreover, in order to better assess the actual stability of the multilayer material we have performed ab initio finite temperature molecular dynamics (AIMD) simulations by considering an isolated trilayer prototype: the time step has been taken as 2.5 fs and atomic velocities have been renormalized to the temperature set at T= 77 K at every 40 time steps. The 12 ps MD simulations have been performed with a sparser 3x2x1 Gamma centred sampling of the BZ.

The electronic structure calculations for the adsorption energy of CO_2, N_2 and H_2O within the pores have been carried out at the "coupled" supermolecular second-order Møller-Plesset perturbation theory (MP2C)[35] level of theory by using the Molpro2012.1 package.[36] Our choice to use the MP2C approach relies on its capability to provide reliable estimations for weakly bound systems such as rare gas–fullerene[37] and -coronene[38] as well as molecule–graphynes' pores,[18,24] at an affordable computational cost. For the graphtriyne pore proto-

type we have considered the following bond lengths,[39] which are those obtained from the periodic DFT calculations: 1.431 Å for the aromatic C-C, 1.231 Å for triple C-C, 1.337 Å for the single C-C between two triple C-C bonds, 1.395 Å for the single C-C connecting aromatic and triple C-C bonds. The size of the C-H ends of the pore prototype is 1.090 Å while C-O, N-N and O-H bond lengths are 1.162, 1.100 and 0.957 Å, respectively. In the case of H_2O, the HOH angle is considered to be 104.5 degrees. The aug-cc-pVTZ[40] basis set has been employed for the pore structures, while the aug-cc-pVQZ[40] basis has been used for the interacting molecules. In the MP2C computations all considered molecular structures are treated as rigid bodies: the atoms composing the investigated graphtriyne prototype are frozen in their initial positions and the molecular configuration of CO_2 (and N_2 and H_2O) is not allowed to relax during the calculations. The interaction energies have been further corrected for the basis set superposition error by the counterpoise method of Boys and Bernardi.[41] The zero point vibrational energy corrections to be added to the binding energies in order to provide an estimation of the adsorption enthalpies at 0 K have been obtained by calculating the vibrational harmonic frequencies for the interaction of the interested molecule placed within an inner pore of the prototype of the multi-layer. The latter have been considered as a rigid substrate and the calculations have been performed at the DFT level of theory by exploiting the PBE functional along with the cc-pVTZ[40] basis set and the latest dispersion contribution correction of Grimme[32] as implemented in the Gaussian 09 code.[42] We have checked that this level of theory provide a good estimation of the involved interaction if compared with the reference MP2C calculations as shown in the Supporting Information, where the case of the molecular interaction with a single pore is reported.

3 Results and Discussion

3.1 Porous graphite structure

The novel graphite we propose is composed of stacked graphtriyne sheets and the accurate assessment of its 3D structure represents a challenging task since the strong interlayer dispersion forces leading to the compact carbon material must be correctly taken into account. To do that we rely on the approach recently introduced by Brandenburg et al.[43] which provides reliable dispersion corrections to periodic DFT calculations: as a matter of fact its application guaranteed accurate and reference values[43] for both exfoliation energy and interlayer separation of pristine graphite. In our previous work[24] the same approach has been used to determine the interlayer equilibrium distance of the graphtriyne bilayer for a specific stacking configuration: we have found it to be 3.45 Å, which is just 0.1 Å larger than that for pristine graphite. Here, we determine in details the energy features of the bilayer relative configuration in order to correctly determine its optimal stacking: this represents a critical point since it could occur that the pore of one layer is partially or totally obstructed by the phenyl ring of the adjacent layer and thus leading to a difficult or impeded diffusion of atoms and molecules through the multi-layer. Accordingly, we have performed DFT calculations for the bilayer interaction energy at a fixed interlayer distance (equals to 3.45 Å) and as a function of the shift of one layer upon the other along two different directions. In the left part of Fig. 1 we report the optimized structure of the 2D graphtriyne monolayer used to perform the periodic DFT calculations of the bilayer interaction: the in-plane lattice parameters are also reported and throughout the calculations they have been considered fixed as well as the in-plane distances between carbon atoms, that is both carbon sheets have been considered as rigid bodies. In the right part of Fig. 1 we show the energy profiles originated from a series of single point calculations related to the parallel displacement of one layer upon the other with respect to a AA-stacked bilayer corresponding to the zero of the abscissae: we can see that for both a and b directions an almost coincident minimum around

1.55 Å is found and the corresponding bilayer configurations, labelled as AB-1 and AB-2, are also represented. The AB-1 configuration recalls that of the typical Bernal stacking of pristine graphite, while the AB-2 one is similar but with a comparable shift in the in-plane perpendicular direction. Similar minima (not reported in Fig.1) have been also found for displacements along directions others than a and b. The binding energies are -1454.2 and 1452.9 meV for the AB-1 and AB-2 configurations, respectively, which correspond to about 30.3 meV/atom, to be compared to 42.9 meV/atom as estimated at same level of theory for a graphene bilayer.[43] Clearly, for a graphtriyne bilayer a decrease of about 30% in the binding energy is found with respect to the graphene counterpart and this can be understood considering that a graphtriyne plane contains a lower density of carbon atoms: in fact, a graphtriyne layer can be thought as the result of replacing one-third of the carbon-carbon bonds in graphene with triple conjugated acetylenic linkages. Also, from Fig. 1 it can be evidenced that further displacements from the main minimimum at 1.55 Å can lead to another less stable one around 3.5-4.0 Å and the barrier to be overcome is not large being about 125.0 meV ($\sim$ 2.6 meV/atom). At non-zero temperatures, these energy features could lead to a not well defined structure for the multi-layer with large in-plane and interlayer displacements. Therefore it is worth further investigating the stability of the 3D structure of by performing DFT/AIMD simulations. To do that we have considered as a starting point two different trilayers in ABA-1 and ABA-2 stackings, which are related to the AB-1 and AB-2 minimum geometries found for the bilayer. Then molecular dynamics simulations are run at constant temperature T= 77K (typical in gas adsorption experiments) for about 12.5 ps and we have found that both starting points eventually lead to a similar ABA structure. Once the system equilibration has been reached (after about 9 ps), radial distributions of both the interlayer distance and inner plane layer displacement have been computed and they are reported in Fig. 2. As for the interlayer distance we have considered the distances between corresponding carbon atoms constituting the phenyl rings lying on the outer layers since during the simulations their relative position on the ab plane remains almost constant.

As for the inner layer shift we have taken into account the relative position on the ab plane of the carbon atoms constituting the phenyl rings with respect to the corresponding ones on the external sheets.

Our results show that the interlayer distance between the outermost layers ranges between 6.7 and 7.1 Å, an interval whose middle point coincides with the double of the equilibrium distance (3.45 Å) we previously found[24] for the bilayer. In the case of the inner layer shift we have found that the most prominent probability is between 1.3 and 1.9 Å, that is around the main minima shown in Fig. 1. These results clearly demonstrate that, despite their weaker interlayer binding with respect to pristine graphite, graphtriyne layers tend to aggregate and to maintain a stable multi-layer structure at finite temperatures: this structure is of a ABA-1 type (see Fig. 1) and the displacement of the inner layer with respect to outer ones is limited. The latter ensures that in the bulk material the free sliding of one layer upon the others is impeded and, more importantly, that the pore of one layer is sligthly displaced from the corresponding ones on the adjacent layers leading to a sort of nano-channels that cross throughout the multi-layer. These nano-channels could be exploited for gas diffusion and adsorption and the in the following we analyze the capability of the novel nano-porous graphite to selectively adsorb CO_2 molecules.

3.2 CO_2 preferential adsorption

First, the interaction between the gas molecule and a graphtriyne single pore is accurately determined. In order to do it, we have considered a molecular precursor of the pore represented by the octadecadehydrotribenzo[24]annulene (Fig. 3, top panel), together with the most stable in-pore configuration of the considered gas molecules, that is CO_2, N_2, H_2O and H_2. In the case of N_2 and CO_2 the optimal geometry is that perpendicular to the pore plane with the center mass of the molecule lying in the geometrical center of the opening; for H_2O and H_2 instead the most favourable geometries are co-planar to the pore as clearly reported in the figure. The molecule configurations are kept frozen during the calculations and they

are those represented in the upper part of Fig. 3. (Additional calculations allowing to fully relax the structure of the involved partners have been also performed to check the reliability of the obtained unrelaxed interactions, as reported in the Supporting Information.) In the lower part of Fig. 3 the corresponding interaction curves obtained at the MP2C level of theory are depicted as a function of the gas molecule distance from the center of the pore. It can be seen that in all cases except for N_2 the minimum is located just inside the pore, that is the size of the opening is large enough to host the considered molecular species; in the case of N_2 the minimum is slightly displaced from the pore plane even if a quite flat minimum centered at about z=0.5 Åcan be observed. Moreover, the largest binding energy corresponds to CO_2 as it could be expected considering that the involved interaction is mostly determined by the van der Waals contribution being the considered pore a neutral and non-polar substrate: in such cases both the dispersion attraction and size repulsion are mainly governed by the molecular dipole polarizability and that of CO_2[44] is the largest among the selected species. The binding energy of CO_2 adsorbed within a graphtriyne pore is about 200 meV and it also slightly larger than the best empirical (178 meV[25]) and theoretical (198 meV[26]) estimates for the physisorption on a graphene plane. A similar trend can also be found for N_2, H_2O and H_2. The results of Fig. 3 show a remarkable preferential adsorption of CO_2 over H_2 within an isolated graphtriyne pore, which suggests a possible application for carbon capture in pre-combustion gas streams; on the contrary the CO_2 binding energy is not sufficiently far from that of H_2O and N_2, and therefore the capability of carbon capture and separation does not seem likely in post-combustion gas mixtures. However, one could expect that the separation between binding energies related to the different species will increase if the adsorption within the pore lying on an inner layer of the multi-layered graphtriyne is taken into account.

In order to verify this hypothesis we have built up a molecular prototype[24] of the nanochannel by considering three parallel graphtriyne pores arranged in a ABA-1 stacking as depicted in the upper part of Fig. 4: by using the geometry parameter determined in the

previous section we have placed the inner pore with a lateral shift of 1.6Å with respect the outer ones, while the adjacent layers are separated by 3.45 Å.

In Fig. 4 the positions of the specific molecule considered for the calculations are also reported and they are indicated in blue as A, B, C, B' and A'. In particular, the A, A' and C sites correspond to in-pore configurations in which the molecule is right in the pore geometric center. B and B' equivalent sites correspond instead to the molecule intercalation: the molecule center of mass lies right in the direction (dashed line) joining the geometric centers of adjacent pores and it is placed at 1.725 Å (half the interlayer distance) from the closest layers. In the lower part of Fig. 4 the adsorption energies obtained at the MP2C level are reported for the five adsorption sites and each value corresponds to the sum of three contributions related to the specific molecule interacting with each of the graphtriyne pore. The intention is to provide the evolution of the adsorption energy as the molecule crosses the nanoporous graphite.

For the in-pore A, A', and C sites the obtained interaction energies are significantly larger than those for the single pore case (see Fig. 3): clearly the largest interaction corresponds to the C case (that for the specific molecule inside the intermediate pore) and the related adsorption energies for CO_2, N_2, and H_2 are more than 50% larger than those for the single pore. The interaction improvement is less evident in the case of H_2O whose adsorption energy increases of about 40%: this could be explained considering that polarization contributions to the global interaction due to the water dipole moment are less effective for the interaction with the outer and indeed farther pores.

As for the B and B' intercalation sites, the interaction energies are more attractive than those for the more external in-pore A and A' locations, even if less than those for the C position.

In general the results reported in Fig. 4 suggest several conclusions. The first point is that no significant hindrance is present for molecule penetration across the multi-layer:in fact, when passing from a pore to the adjacent one along the z direction no relevant barrier

(that is the energy difference between the C and B sites) is observed. This means that the out-of-plane gas diffusion through the novel porous graphite could be possible.

Interestingly, in the case of CO_2 the energy difference between the A and B sites is more pronounced (more than 50 meV) than that for the other species suggesting that once the molecule is hosted inside the material its release would be more difficult.

The second point to highlight is that a quite favourable binding energy (about 310 meV) is found for CO_2 within the inner pore and also that it is about 100 meV larger than those for H_2O and N_2. The differences between the binding energy values corresponding to the inner pore can be roughly understood by considering the dipole polarizabilities[44] of the physisorbed molecules, as already anticipated above in the case of the results for the interaction with a single pore. In particular, it can be checked that for the non-polar CO_2, N_2, and H_2 species the ratio of the molecular dipole polarizabilities roughly corresponds to that of the related binding energies: as an example, for CO_2/N_2 (CO_2/H_2) the polarizability (α) ratio is 1.47 (3.19) while the energy one is 1.54 (3.24). However, in the case of CO_2/H_2O this rule of thumb predicts for H_2O a binding energy lower than that for N_2 since $\alpha_{H_2O} < \alpha_{N_2}$[44] but this trend is just the opposite of that shown in Fig. 4. As a matter of fact, H_2O is a polar molecule and induction effects provoked by its permanent electric dipole moment must be taken into account which lead to further attractive interactions. The latters sum to the ubiquitous dispersion interactions which instead can be described by just considering the polarizabilities of the involved partners.

In order to better assess the preferential adsorption of CO_2 an estimation of the adsorption enthalpies, which represent more realistic magnitudes for the single molecule–substrate interactions here investigated, have been also computed. To do that zero point vibrational energy (ZPVE) corrections have been calculated at the DFT level of theory within a harmonic vibration approximation: we have assumed the substrate as a rigid body and we have optimized the position of the adsorbed molecule whose internal coordinates have been also relaxed. The obtained ZPVE corrections have been then added to the MP2C binding

energies to obtain an approximation of the adsorption enthalpies at 0 K. (All the results are summarized in Table 1). It is straightforward that the adsorption enthalpy of CO_2 is significantly larger than those of the other considered species: the energy difference ranges from about 235 meV for H_2 to 110 meV for H_2O and N_2. These data suggest that a preferential adsorption of CO_2 over H_2, H_2O, and N_2 could be expected within the pores of the novel nanoporous graphite. These feautures, together with a moderate adsorption enthalpy for CO_2 (about 300 meV), which entails a strong physisorption, promote the new carbon layered material as an efficient adsorbing medium not only for pre-combustion capture processes but also for those involved in post-combustion where wet CO_2/N_2 mixtures have to be treated.

As an example, on the basis of stoichiometric considerations and assuming that one CO_2 molecules could be hosted in each pore we can provide an estimation of the related gravimetric storage capacity of about 5.3 $\mathrm{mmol\,g^{-1}}$ (23.4 wt%), which is in the range or even higher than those for the best carbon adsorbing materials to date[5,6,10] at low pressures ($\sim$ 1 bar), which are those of interest in post-combustion flue gas. Indeed, the uniformly distributed sub-nanometer triangular pores featuring the novel graphite are expected to provide good uptake performances at atmospheric and lower pressures since it has been found[45] that at such conditions the CO_2 sorption is mostly determined by pores with diameter smaller than 0.8 nm.

4 Conclusions

In summary, by means of electronic structure and molecular dynamics computations, we have shown that graphtriyne layers tend to associate themselves at finite temperatures to form stable layered structures representing a new kind of porous graphite. The optimal structures have been identified and they correspond to ABA-like stackings with an average interlayer separation of about 3.45 Å; moreover we have shown that the displacement of

one layer with respect the adjacent ones is limited ($\sim$ 1.6 Å) allowing the spatial connection between corresponding pores lying on different sheets and leading to a sort of nanochannels which perpendicularly cross the 3D material. We have shown that these nanochannels are large enough to host light gases such as CO_2, N_2, H_2O and H_2 allowing also their diffusion. The corresponding adsorption energies and enthalpies have been computed: a strong physisorption is found for CO_2 and a significant selectivity is expected over the other considered species which could be exploited in both pre- and post-combustion carbon capture techniques.

The novel porous graphite we propose could be considered as a promising alternative to more traditional adsorbing materials based on carbon; as most of them it is hydrophobic, chemically inert and thermally stable but with the advantage of a very compact cristallyne structure with regular pores uniformly distributed and of sub-nanometer size, which are especially suited to host light gas species.

Acknowledgments

The work has been funded by the Spanish grant FIS2013-48275-C2-1-P. Allocation of computing time by CESGA (Spain) is also acknowledged.

Supplementary Material

Intermolecular potentials obtained at the DFT level of theory for the molecule–graphtriyne pore interaction are reported in an additional figure and table which provide validations of both the DFT approach used to estimate zero point corrections and the rigid bodies approximation used to calculate interaction energies. This information is available free of charge via the Internet.

References

(1) Lackner, K. S.; Brennan, S.; Matter, J.; Park, A.-H. A.; Wright, A.; van der Zwaan, B. The Urgency of the Development of CO_2 Capture from Ambient Air. *Proc. Natl. Acad. Sci. U. S. A.* **2012**, *109*, 13156–13162.

(2) Scott, V.; Gilfillan, S.; Markusson, N.; Chalmers, H.; Haszeldine, R. S. Last Chance for Carbon Capture and Storage. *Nat. Clim. Change* **2013**, *3*, 105–111.

(3) Broom, D. P.; Thomas, K. M. Gas Adsorption by Nanoporous Materials: Future Applications and Experimental Challenges. *MRS Bull.* **2013**, *38*, 412–420.

(4) Makal, T. A.; Li, J. R.; Lu, W.; Zhou, H. C. Methane Storage in Advanced Porous Materials. *Chem. Soc. Rev.* **2012**, *41*, 7761–7779.

(5) Nandi, M.; Uyama, H. Exceptional CO2 Adsorbing Materials under Different Conditions. *Chem. Rec.* **2014**, *14*, 1134–1148.

(6) Gadipelli, S.; Vaiva, K.; Zheng-Xiao, G.; Taner, Y. Exceptional CO2 Capture in a Hieararchically Porous Carbon with Simultaneous High Surface Area and Pore Volume. *Energy Environ. Sci.* **2014**, *7*, 335–342.

(7) Balasubramanian, R.; Chowdhury, S. Recent Advances and Progress in the Development of Graphene-Based Adsorbents for CO2 Capture. *J. Mater. Chem. A* **2015**, *3*, 21968–21989.

(8) Burress, J. W.; Gadipelli, S.; Ford, J.; Simmons, J. M.; Zhou, W.; Yildirim, T. Graphene Oxide Framework Materials: Theoretical Predictions and Experimental Results. *Angew. Chem., Int. Ed.* **2010**, *49*, 8902–8904.

(9) Klechikov, A. G.; Mercier, G.; Merino, P.; Blanco, S.; Merino, C.; Talyzin, A. V. Hydrogen Storage in Bulk Graphene-related Materials. *Microporous Mesoporous Mater.* **2015**, *210*, 46–51.

(10) Ganesan, A.; Shaijumon, M. M. Activated Graphene-derived Porous Carbon with Exceptional Gas Adsorption Properties. *Microporous Mesoporous Mater.* **2016**, *220*, 21–27.

(11) Bieri, M.; Treier, M.; Cai, J.; Aït-Mansour, K.; Ruffieux, P.; Gröning, O.; Gröning, P.; Kastler, M.; Rieger, R.; Feng, X.; Müllen, K.; Fasel, R. Porous Graphenes: Two-dimensional Polymer Synthesis with Atomic Precision. *Chem. Commun.* **2009**, *45*, 6919–6921.

(12) Li, G.; Li, Y.; Liu, H.; Guo, Y.; Li, Y.; Zhu, D. Architecture of Graphdiyne Nanoscale Films. *Chem. Commun.* **2010**, *46*, 3256–3258.

(13) Narita, N.; Nagai, S.; Suzuki, S.; Nakao, K. Optimized Geometries and Electronic Structures of Graphyne and Its Family. *Phys. Rev. B* **1999**, *58*, 11009–11014.

(14) Li, Y.; Xu, L.; Liu, H.; Li, Y. Graphdiyne and Graphyne: from Theoretical Predictions to Practical Construction. *Chem. Soc. Rev.* **2014**, *43*, 2572–2586.

(15) Zhou, J.; Gao, X.; Liu, R.; Xie, Z.; Yang, J.; Zhang, S.; Zhang, G.; Liu, H.; Li, Y.; Zhang, J.; Liu, Z. Synthesis of Graphdiyne Nanowalls Using Acetylenic Coupling Reaction. *J. Am. Chem. Soc.* **2015**, *137*, 7596–7599.

(16) Cranford, S. W.; Buehler, M. J. Selective Hydrogen Purification Through Graphdiyne Under Ambient Temperature and Pressure. *Nanoscale* **2012**, *4*, 4587–4593.

(17) Lin, S.; Buehler, M. J. Mechanics and Molecular Filtration Performance of Graphyne Nanoweb Membranes for Selective Water Purification. *Nanoscale* **2013**, *5*, 11801–11807.

(18) Bartolomei, M.; Carmona-Novillo, E.; Hernández, M. I.; Campos-Martínez, J.; Pirani, F.; Giorgi, G.; Yamashita, K. Penetration Barrier of Water through Graphynes' Pores: First-Principles Predictions and Force Field Optimization. *J. Phys. Chem. Lett.* **2014**, *5*, 751–755.

(19) Bartolomei, M.; Carmona-Novillo, E.; Hernández, M. I.; Campos-Martínez, J.; Pirani, F.; Giorgi, G. Graphdiyne Pores: "Ad Hoc" Openings for Helium Separation Applications. *J. Phys. Chem. C* **2014**, *118*, 29966–29972.

(20) Hernández, M. I.; Bartolomei, M.; Campos-Martínez, J. Transmission of Helium Isotopes through Graphdiyne Pores: Tunneling versus Zero Point Energy Effects. *J. Phys. Chem. A* **2015**, *119*, 10743–10749.

(21) Zheng, Q.; Luo, G.; Liu, Q.; Quhe, R.; Zheng, J.; Tang, K.; Gao, Z.; Nagase, S.; Lu, J. Structural and Electronic Properties of Bilayer and Trilayer Graphdiyne. *Nanoscale* **2012**, *4*, 3990–3996.

(22) Decéré, J.; Lepetit, C.; Chauvin, R. Carbo-graphite: Structural, Mechanical, and Electronic Properties. *J. Phys. Chem. C* **2013**, *117*, 21671–21681.

(23) Luo, G.; Zheng, Q.; Mei, W.; Lu, J.; Nagase, S. Structural, Electronic, and Optical Properties of Bulk Graphdiyne. *J. Phys. Chem. C* **2013**, *117*, 13072–13079.

(24) Bartolomei, M.; Carmona-Novillo, E.; Giorgi, G. First Principles Investigation of Hydrogen Physical Adsorption on Graphynes' Layers. *Carbon* **2005**, *95*, 1076–1081.

(25) Vidali, G.; Ihm, G.; Kim, H. Y.; Cole, M. W. Potentials of Physical Adsorption. *Surf. Sci. Rep.* **1991**, *12*, 133–181.

(26) Rubes, M.; Kysilka, J.; Nachtigall, P.; Bludsky, O. DFT/CC Investigation of Physical Adsorption on a Graphite (0001) Surface. *Phys. Chem. Chem. Phys.* **2010**, *12*, 6438–6444.

(27) Silvestrelli, P. L.; Ambrosetti, A. Including Screening in van der Waals Corrected Density Functional Theory Calculations: The case of Atoms and Small Molecules Physisorbed on Graphene. *J. Chem. Phys.* **2014**, *140*, 124107.

(28) Kresse, G.; Furthmüller, J. Efficient Iterative Schemes for Ab Initio Total-Energy Calculations Using a Plane-Wave Basis Set. *Phys. Rev. B* **1996**, *54*, 11169–11186.

(29) Perdew, J.; Burke, K.; Ernzerhof, M. Generalized Gradient Approximation Made Simple. *Phys. Rev. Lett.* **1996**, *77*, 3865–3868.

(30) Blöchl, P. Projector Augmented-Wave Method. *Phys. Rev. B* **1994**, *50*, 17953–17979.

(31) Kresse, G.; Joubert, D. From Ultrasoft Pseudopotentials to the Projector Augmented-Wave Method. *Phys. Rev. B* **1999**, *59*, 1758–1775.

(32) Grimme, S.; Ehrlich, S.; Goerigk, L. Effect of the Damping Function in Dispersion Corrected Density Functional Theory. *J. Comput. Chem.* **2011**, *32*, 1456–1465.

(33) Brandenburg, J. G.; Hochheim, M.; Bredow, T.; Grimme, S. Low-Cost Quantum Chemical Methods for Noncovalent Interactions. *J. Phys. Chem. Lett.* **2014**, *5*, 4275–4284.

(34) Grimme, S.; Antony, J.; Ehrlich, S.; Krieg, H. A consistent and Accurate Ab Initio Parametrization of Density Functional Dispersion Correction (DFT-D) for the 94 Elements H-Pu. *J. Chem. Phys.* **2010**, *132*, 154104.

(35) Pitonák, M.; Hesselmann, A. Accurate Intermolecular Interaction Energies from a Combination of MP2 and TDDFT Response Theory. *J. Chem. Theory Comput.* **2010**, *6012*, 168–178.

(36) Werner, H.-J.; Knowles, P. J.; Lindh, R.; Manby, F. R.; Schütz, M.; Celani, P.; Korona, T.; Rauhut, G.; Amos, R. D.; Bernhardsson, A.; Berning, A.; Cooper, D. L.; Deegan, M. J. O.; Dobbyn, A. J.; Eckert, F.; Hampel, C.; Hetzer, G.; Lloyd, A. W.; McNicholas, S. J.; Meyer, W.; Mura, M. E.; Nicklass, A.; Palmieri, P.; Pitzer, R.; Schumann, U.; Stoll, H.; Stone, A. J.; Tarroni, R.; Thorsteinsson, T. MOLPRO, Version2012.1, a Package of Ab Initio Programs. 2012; seehttp://www.molpro.net.

(37) Hesselmann, A.; Korona, T. On the Accuracy of DFT-SAPT, MP2, SCS-MP2, MP2C, and DFT+DISP Methods for the Interaction Energies of Endohedral Complexes of the C(60) Fullerene with a Rare Gas Atom. *Phys. Chem. Chem. Phys.* **2011**, *13*, 732–743.

(38) Bartolomei, M.; Carmona-Novillo, E.; Hernández, M. I.; Campos-Martínez, J.; Pirani, F. Global Potentials for the Interaction Between Rare Gases and Graphene-Based Surfaces: An Atom-Bond Pairwise Additive Representation. *J. Phys. Chem. C* **2013**, *117*, 10512–10522.

(39) Pei, Y. Mechanical Properties of Graphdiyne Sheet. *Physica B* **2012**, *407*, 4436–4439.

(40) Kendall, R. A.; Dunning, T. H.; Harrison, R. J. Electron Affinities of the First-Row Atoms Revisited. Systematic Basis Sets and Wave Functions. *J. Chem. Phys.* **1992**, *96*, 6796–6806.

(41) Boys, S.; Bernardi, F. The Calculation of Small Molecular Interactions by the Differences of Separate Total Energies. Some Procedures with Reduced Errors. *Mol. Phys.* **1970**, *19*, 553–566.

(42) Frisch, M. J.; Trucks, G. W.; Schlegel, H. B.; Scuseria, G. E.; Robb, M. A.; Cheeseman, J. R.; Scalmani, G.; Barone, V.; Mennucci, B.; Petersson, G. A.; Nakatsuji, H.; Caricato, M.; Li, X.; Hratchian, H. P.; Izmaylov, A. F.; Bloino, J.; Zheng, G.; Sonnenberg, J. L.; Hada, M.; Ehara, M.; Toyota, K.; Fukuda, R.; Hasegawa, J.; Ishida, M.; Nakajima, T.; Honda, Y.; Kitao, O.; Nakai, H.; Vreven, T.; Montgomery, J. A., Jr.; Peralta, J. E.; Ogliaro, F.; Bearpark, M.; Heyd, J. J.; Brothers, E.; Kudin, K. N.; Staroverov, V. N.; Kobayashi, R.; Normand, J.; Raghavachari, K.; Rendell, A.; Burant, J. C.; Iyengar, S. S.; Tomasi, J.; Cossi, M.; Rega, N.; Millam, J. M.; Klene, M.; Knox, J. E.; Cross, J. B.; Bakken, V.; Adamo, C.; Jaramillo, J.; Gomperts, R.; Stratmann, R. E.; Yazyev, O.; Austin, A. J.; Cammi, R.; Pomelli, C.; Ochterski, J. W.; Martin, R. L.; Morokuma, K.; Zakrzewski, V. G.; Voth, G. A.; Salvador, P.; Dannen-

berg, J. J.; Dapprich, S.; Daniels, A. D.; Farkas, O.; Foresman, J. B.; Ortiz, J. V.; Cioslowski, J.; Fox, D. J. Gaussian 09 Revision E.01. Gaussian Inc. Wallingford CT 2009.

(43) Brandenburg, J. G.; Alessio, M.; Civalleri, B.; Peintinger, M. F.; Bredow, T.; Grimme, S. Geometrical Correction for the Inter- and Intramolecular Basis Set Superposition Error in Periodic Density Functional Theory Calculations. *J. Phys. Chem. A* **2013**, *117*, 9282–9292.

(44) Olney, T. N.; Cann, N.; Cooper, G.; Brion, C. Absolute Scale Determination for Photoabsorption Spectra and the Calculation of Molecular Properties Using Dipole Sum-rules. *Chem. Phys.* **1997**, *223*, 59–98.

(45) Presser, V.; McDonough, J.; Yeon, S. H.; Gogotsi, Y. Effect of Pore Size on Carbon Dioxide Sorption by Carbide Derived Carbon. *Energy Environ. Sci.* **2011**, *4*, 3059–3066.

Table 1: Binding energies, zero point vibrational energy corrections and adsorption enthalpies for a single molecule hosted within an inner pore of the porous graphite (see Fig. 4). All values are in meV.

	Binding energy[a]	ZPVE[b]	Δ_{ads}H(0 K)
CO_2	312.0	12.7	-299.3
H_2O	224.3	32.4	-191.8
N_2	203.0	14.3	-188.7
H_2	96.4	31.6	-64.8

[a] From MP2C computations. [b] From harmonic frequency calculations at the DFT level of theory assuming the pores as rigid structures and allowing the internal coordinates of the adsorbed species to relax.

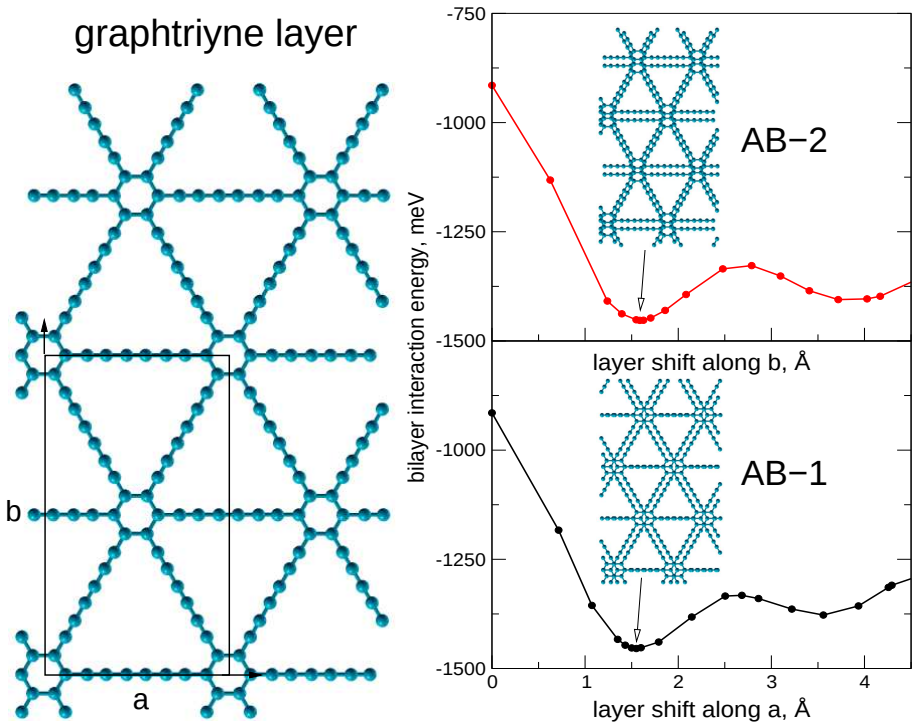

Figure 1: Left part: Top view of the supercell describing the graphtriyne layer used in the periodic DFT calculations together with a and b lattice parameters. Right part: bilayer interaction energy (relative to the asymptotic layer separation) as a function of the shift of one layer upon the other along the a (lower panel) and b (upper panel) directions. The interlayer distance has been kept fixed at 3.45 Å and the shift is measured with respect to the least favourable AA stacking, that is with carbon atoms on both layers having the same coordinates along a and b. The most favourable bilayer structures are also reported in each panel and labelled as AB-1 and AB-2.

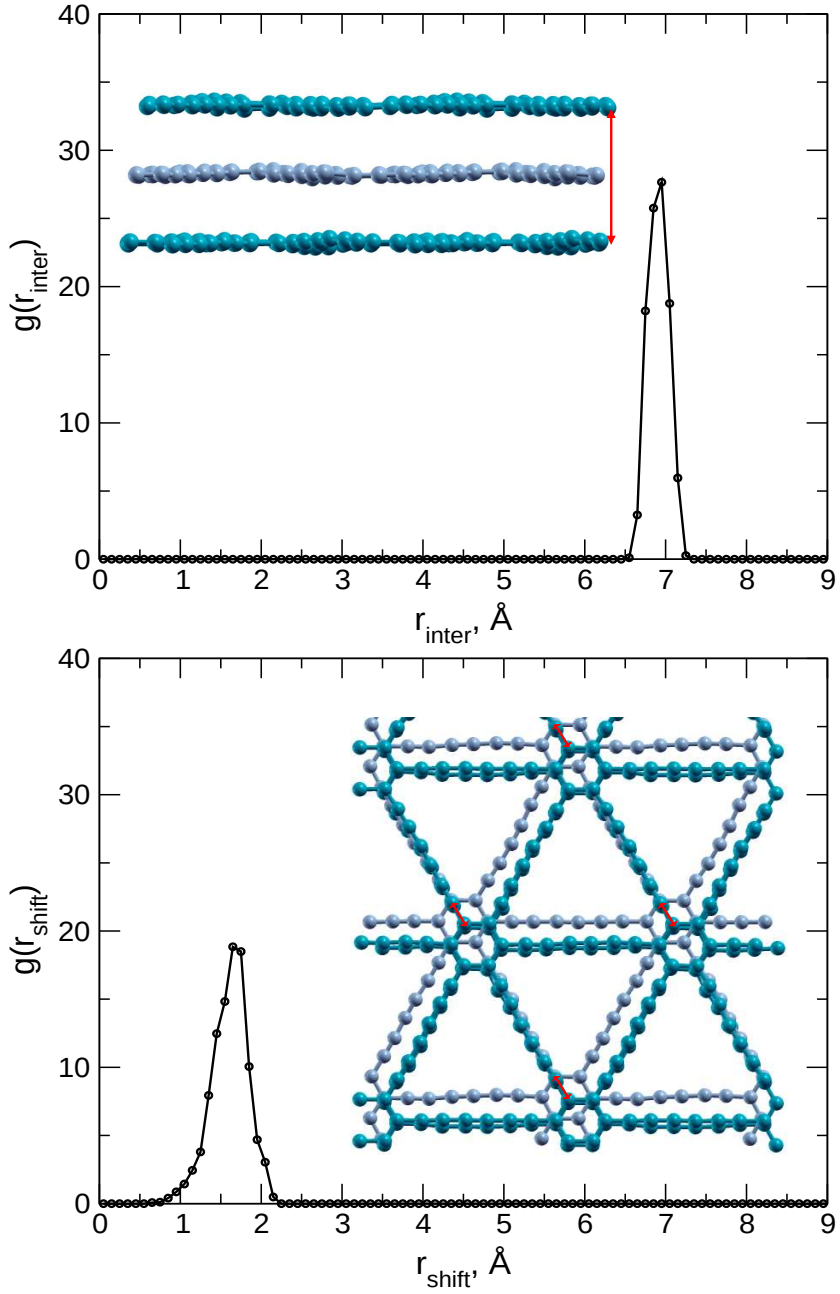

Figure 2: Graphtriyne trilayer: radial distributions of the interlayer distance between the outer layers (upper panel) and of the inner layer displacement (lower panel) with respect to the external ones. Side and top views of the structure obtained after molecular dynamics equilibration are also reported in the upper and lower panel, respectively. The inner layer is shown in grey for the sake of a better visibility. The red double-headed arrows provide graphical representations of the interlayer distance and inner layer shift.

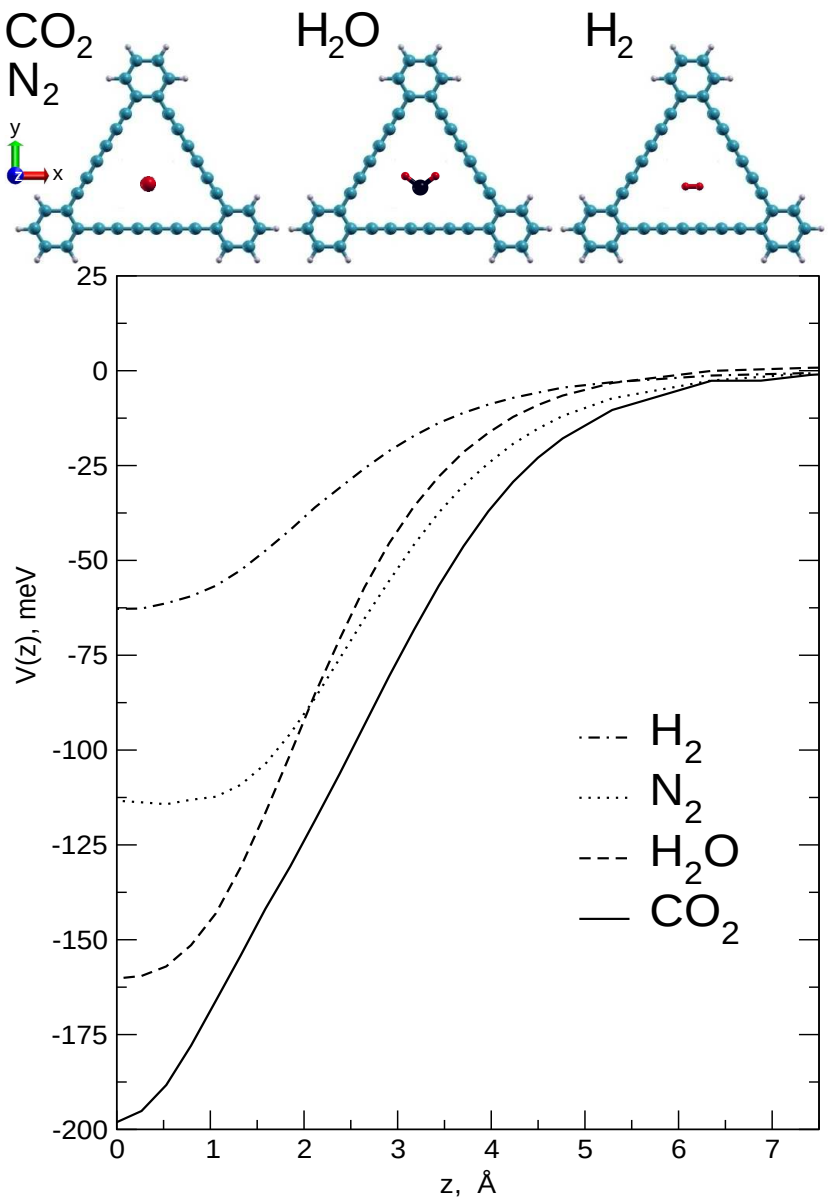

Figure 3: Upper part: CO_2, N_2, H_2O and H_2 optimal in-pore configuration for their interaction with a graphtriyne pore represented by its smallest molecular precursor. CO_2 and N_2 are in a perpendicular geometry with respect to the planar opening while H_2O and H_2 lie in a coplanar arrangement. Lower part: adsorption energy profiles for the specific molecule obtained at the MP2C level of theory as a function of z, the distance from the molecule center of mass to the geometric center of the pore. Throughout the calculation the relative configuration of the molecule-pore complex is kept frozen as in the corresponding one shown in the upper part and the internal coordinates of the monomers are not allowed to relax.

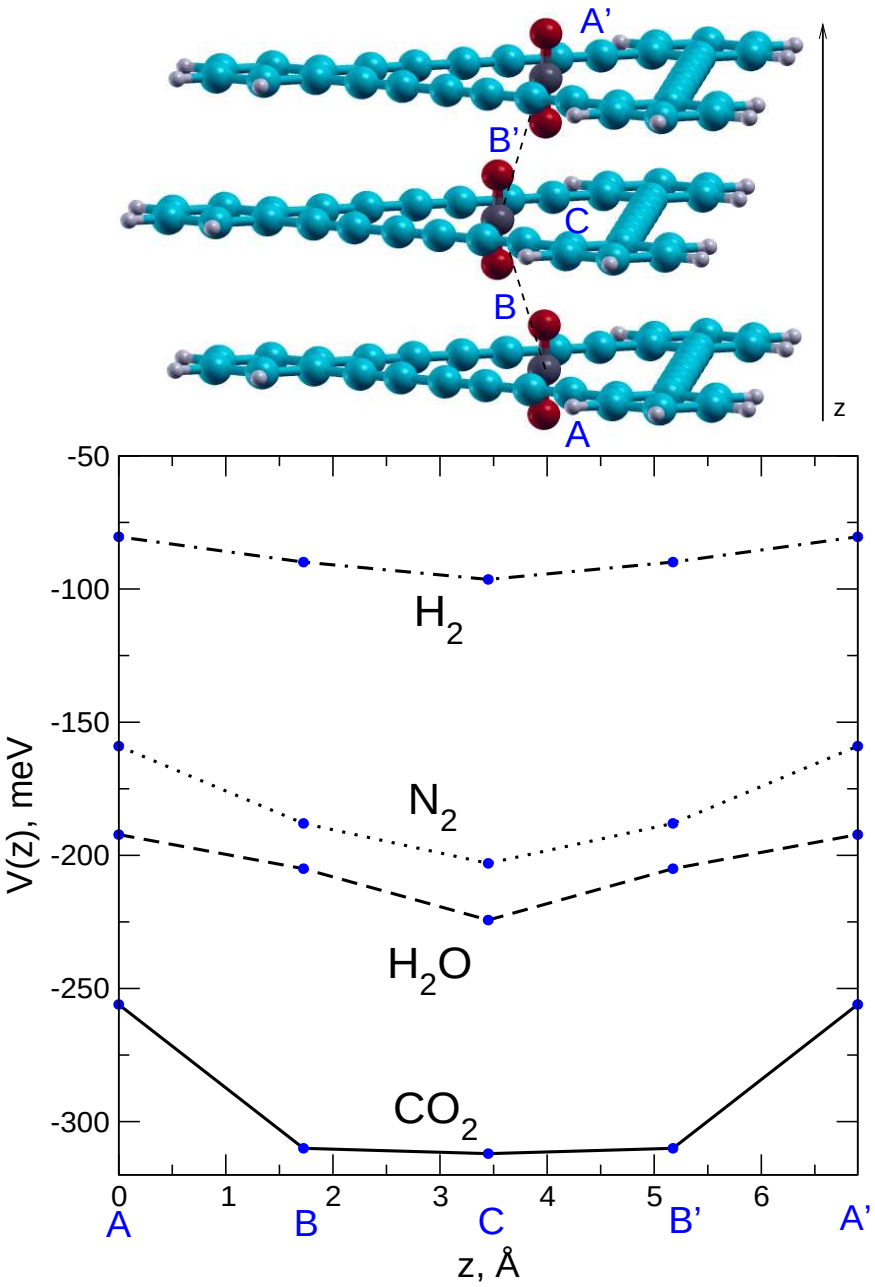

Figure 4: Interaction energy evolution of the CO_2, H_2O, N_2, and H_2 molecules crossing the nanoporous graphite. A prototype consisting of three parallel graphtriyne pores in ABA-1 arrangement is used. The A, A', B, B' and C letters indicate different adsorption sites within the multi-layer: A, A' and C locations correspond to in-pore configurations while B and B' sites to intercalation equivalent positions. The five adsorption sites lie on the dashed lines which join the geometric centers of adjacent pores; the layers separation is fixed at 3.45 Å while the displacement of the inner pore is fixed at 1.6 Å, the geometry parameters provided by the calculations shown in Fig. 2.